26

Robust Vehicle Stability Control Based on Sideslip Angle Estimation

Haiping Du[1] and Nong Zhang[2]
[1]*School of Electrical, Computer and Telecommunications Engineering*
University of Wollongong, Wollongong, NSW 2522
[2]*Mechatronics and Intelligent Systems, Faculty of Engineering*
University of Technology, Sydney, P.O. Box 123, Broadway, NSW 2007
Australia

1. Introduction

Vehicle stability control is very important to vehicle active safety, in particular, during severe driving manoeuvres. The yaw moment control has been regarded as one of the most promising means of vehicle stability control, which could considerably enhance vehicle handling and stability (Abe, 1999; Mirzaei, 2010). Up to the date, different strategies on yaw moment control, such as optimal control (Esmailzadeh et al., 2003; Mirzaei et al., 2008), fuzzy logic control (Boada et al, 2005; Li & Yu 2010), internal model control (IMC) (Canale et al., 2007), flatness-based control (Antonov et al, 2008), and coordinated control (Yang et al, 2009), etc., have been proposed in the literature.

It is noticed that most existing yaw moment control strategies rely on the measurement of both sideslip angle and yaw rate. However, the measurement of sideslip angle is hard to be done in practice because the current available sensors for sideslip angle measurement are all too expensive to be acceptable by customers. To implement yaw moment controller without increasing too much cost on a vehicle, the estimation of sideslip angle based on measurement available signals, such as yaw rate and lateral acceleration, etc., is becoming necessary. And, the measurement noise should also be considered so that the estimation based controller is more robust. On the other hand, most of the existing studies use a linear lateral dynamics model with nominal cornering stiffness for the yaw moment controller design. Since the yaw moment control obviously relies on the tyre lateral force and the tyre force strongly depends on tyre vertical load and road conditions which are very sensitive to the vehicle motion and the environmental conditions, the tyre cornering stiffness must have uncertainties. Taking cornering stiffness uncertainties into account will make the controller being more robust to the variation of road conditions. In addition, actuator saturation limitations resulting from some physical constraints and tyre-road conditions must be considered so that the implementation of the controller can be more practical.

In this chapter, a nonlinear observer based robust yaw moment controller is designed to improve vehicle handling and stability with considerations on cornering stiffness uncertainties, actuator saturation limitation, and measurement noise. The yaw moment

controller uses the measurement of yaw rate and the estimation of sideslip angle as feedback signals, where the sideslip angle is estimated by a Takagi-Sugeno (T-S) fuzzy model-based observer. The design objective of this observer based controller is to achieve optimal performance on sideslip angle and estimation error subject to the cornering stiffness uncertainties, actuator saturation limitation, and measurement noise. The design of such an observer based controller is implemented in a two-step procedure where linear matrix inequalities (LMIs) are built and solved by using available software Matlab LMI Toolbox. Numerical simulations on a vehicle model with nonlinear tyre model are used to validate the control performance of the designed controller. The results show that the designed controller can achieve good performance on sideslip angle responses for a given actuator saturation limitation with measurement noise under different road conditions and manoeuvres.

This chapter is organised as follows. In Section 2, the vehicle lateral dynamics model is introduced. The robust observer-based yaw moment controller design is introduced in Section 3. In Section 4, the simulation results on a nonlinear vehicle model are discussed. Finally, conclusions are presented in Section 5.

The notation used throughout the paper is fairly standard. For a real symmetric matrix M the notation of $M>0$ ($M<0$) is used to denote its positive- (negative-) definiteness. $\|.\|$ refers to either the Euclidean vector norm or the induced matrix 2-norm. I is used to denote the identity matrix of appropriate dimensions. To simplify notation, * is used to represent a block matrix which is readily inferred by symmetry.

2. Vehicle dynamics model

In spite of its simplicity, a bicycle model of vehicle lateral dynamics, as shown in Fig. 1, can well represent vehicle lateral dynamics with constant forward velocity and is often used for controller design and evaluation.

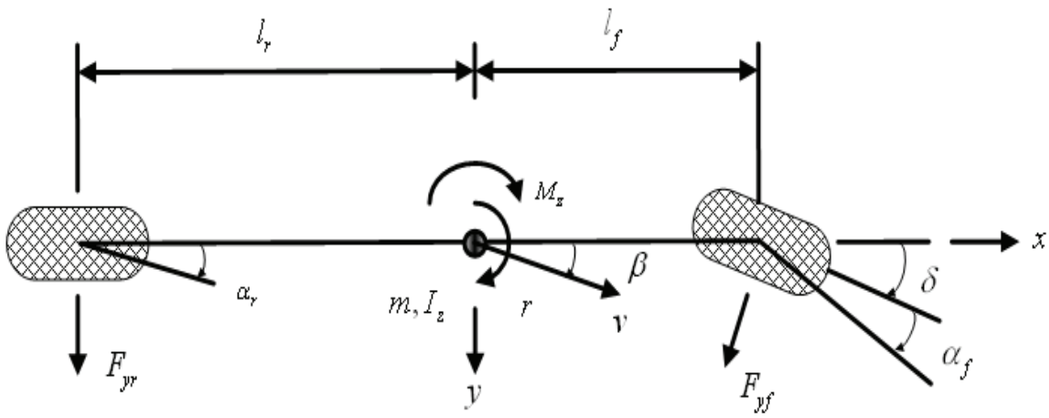

Fig. 1. Vehicle lateral dynamics model

In this model, the vehicle has mass m and moment of inertia I_z about yaw axis through its center of gravity (CG). The front and rear axles are located at distances l_f and l_r, respectively, from the vehicle CG. The front and rear lateral tyre forces F_{yf} and F_{yr} depend on slip angles α_f and α_r, respectively, and the steering angle δ changes the heading of the front tyres.

When lateral acceleration is lower, the tyres operate in the linear region and the lateral forces at the front and rear can be related to slip angles by the cornering stiffnesses of the front and rear tyres as

$$F_{yf}=-C_{\alpha f}\alpha_f, \qquad F_{yr}=-C_{\alpha r}\alpha_r \tag{1}$$

where $C_{\alpha f}$ and $C_{\alpha r}$ are cornering stiffnesses of the front and rear tyres, respectively. With using Newton law and the following relationships

$$\alpha_f=\beta+\frac{l_f r}{v}-\delta, \qquad \alpha_r=\beta-\frac{l_r r}{v} \tag{2}$$

vehicle lateral dynamics model can be written in state space equation as

$$\begin{bmatrix}\dot{\beta}\\ \dot{r}\end{bmatrix}=\begin{bmatrix}-\frac{C_{\alpha f}+C_{\alpha r}}{mv} & -1-\frac{l_f C_{\alpha f}-l_r C_{\alpha r}}{mv^2}\\ -\frac{l_f C_{\alpha f}-l_r C_{\alpha r}}{I_z} & -\frac{l_f^2 C_{\alpha f}-l_r^2 C_{\alpha r}}{I_z v}\end{bmatrix}\begin{bmatrix}\beta\\ r\end{bmatrix}+\begin{bmatrix}\frac{C_{\alpha f}}{mv}\\ \frac{l_f C_{\alpha f}}{I_z}\end{bmatrix}\delta+\begin{bmatrix}0\\ \frac{1}{I_z}\end{bmatrix}M_z \tag{3}$$

where β is vehicle sideslip angle, r is yaw rate, M_z is yaw moment, v is forward velocity. Equation (3) can be further written as

$$\dot{x}=Ax+B_1 w+B_2\bar{u} \tag{4}$$

where

$$A=\begin{bmatrix}-\frac{C_{\alpha f}+C_{\alpha r}}{mv} & -1-\frac{l_f C_{\alpha f}-l_r C_{\alpha r}}{mv^2}\\ -\frac{l_f C_{\alpha f}-l_r C_{\alpha r}}{I_z} & -\frac{l_f^2 C_{\alpha f}-l_r^2 C_{\alpha r}}{I_z v}\end{bmatrix},\ B_1=\begin{bmatrix}\frac{C_{\alpha f}}{mv}\\ \frac{l_f C_{\alpha f}}{I_z}\end{bmatrix}$$
$$B_2=\begin{bmatrix}0\\ \frac{1}{I_z}\end{bmatrix},\ x=\begin{bmatrix}\beta\\ r\end{bmatrix},\ w=\delta,\ u=M_z \tag{5}$$

and

$$\bar{u}=\text{sat}(u)=\begin{cases}-u_{lim} & \text{if } u<-u_{lim}\\ u & \text{if } -u_{lim}\le u\le u_{lim}\\ u_{lim} & \text{if } u>u_{lim}\end{cases} \tag{6}$$

which is used to define the saturation state of control input and u_{lim} is the limitation of available yaw moment in practice.

It is noticed that the linear relationship between tyre lateral force and slip angle in equation (1) can only exist when lateral acceleration is lower (less than about 0.4 g). When lateral acceleration increases, the relationship goes into nonlinear region as shown in Fig. 2 where change of lateral tyre force to sideslip angle generated from Dugoff tyre model is depicted.

Therefore, cornering stiffnesses are no longer constant values but time-varying variables, and relationship between tyre lateral force and slip angle is a nonlinear function of sideslip angle. To describe this nonlinear relationship, cornering stiffnesses need to be measured or estimated. However, either way is difficult to be implemented due to cost or accuracy consideration although some approaches have been proposed for the estimation of cornering stiffnesses.

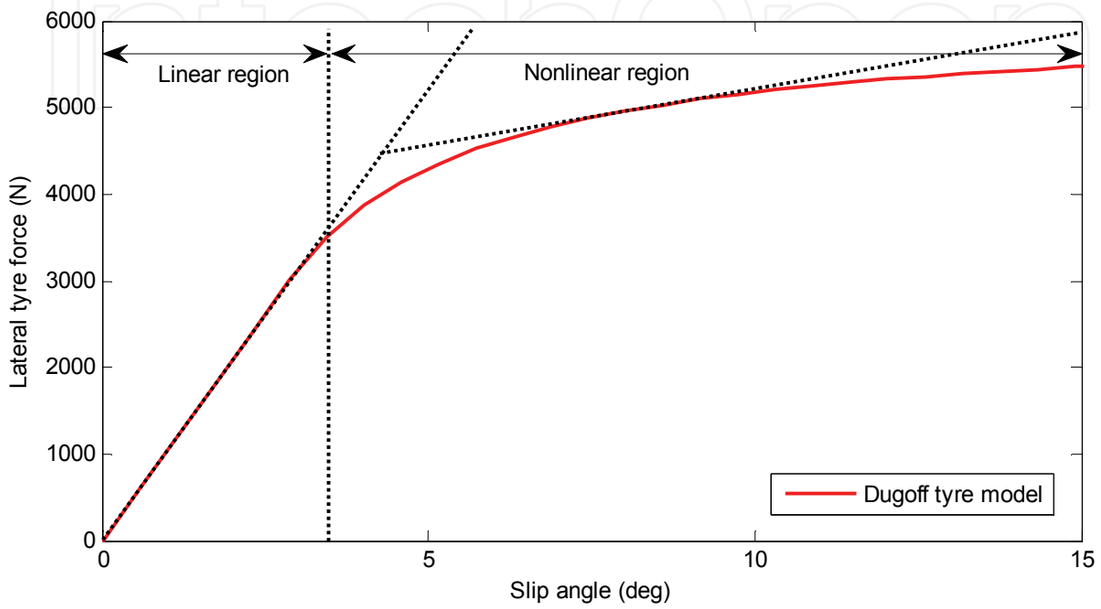

Fig. 2. Tyre lateral force characteristics.

Since Takagi-Sugeno (T-S) fuzzy model has been effectively applied to approximate nonlinear functions in many different applications (Tanaka & Wang, 2001), instead of estimating cornering stiffness, we use T-S fuzzy model to describe the nonlinear relationship between tyre lateral force and sideslip angle in the vehicle lateral dynamics model. The plant rules for the T-S fuzzy lateral dynamics model are built as

IF Δr is N_1 THEN

$$\dot{x}=A_1x+B_{11}w+B_2\bar{u} \tag{7}$$

IF Δr is N_2 THEN

$$\dot{x}=A_2x+B_{12}w+B_2\bar{u} \tag{8}$$

where N_1 and N_2 are fuzzy sets, Δr is premise variable which is defined by deviation of yaw rate as

$$\Delta r=\left[1+\left(\frac{v}{v_c}\right)^2\right]\frac{(r_{ref}-r)l}{v}\frac{|r|}{r} \tag{9}$$

where v_c is characteristic velocity, $l=l_f+l_r$, and the reference yaw rate r_{ref} is defined as

$$r_{ref}=\frac{v}{l}\frac{\delta}{1+\left(\frac{v}{v_c}\right)^2} \tag{10}$$

The deviation of yaw rate is used as a premise variable in this T-S fuzzy model because it can approximately show the degree of nonlinear state and can be used to judge whether the vehicle is in linear or nonlinear region (Fukada, 1999).
By fuzzy blending, the final output of the T-S fuzzy model is inferred as follows

$$\dot{x}=\sum_{i=1}^{2}h_i(\Delta r)\left(A_i x+B_{1i}w+B_2\bar{u}\right) \tag{11}$$

where $h_i(\Delta r)=\mu_i(\Delta r)/\sum_{i=1}^{2}\mu_i(\Delta r)$, $\mu_i(\Delta r)$ is the degree of the membership of Δr in N_i. In general, triangular membership function can be used for fuzzy set N_i, and we have $h_i(\Delta r)\geq 0$ and $\sum_{i=1}^{2}h_i(\Delta r)=1$. A_i and B_{1i} are sub-matrices which are obtained by substituting cornering stiffness values for linear and nonlinear regions, respectively.

3. Observer based robust controller design

It was pointed in many previous research works that both sideslip angle and yaw arte are useful information for effective vehicle handling and stability control. However, sensors for measuring sideslip angle are really expensive and cannot be used in stability control for commercial automotives. Therefore, estimation of slip angle is a cost-effective way to solve this problem. On the contrary, measurement of yaw rate is relatively easy and cheap, and gyroscopic sensor can be used to do it. Base on the measurable yaw rate signal, sideslip angle can be estimated and then used for full state feedback control signal.
In a real application, the state measurements can not be perfect. Thus, the measured state variables should be corrupted by measurement noises as

$$y=Cx+n \tag{12}$$

where y is the measured output, n denotes the measurement noise, C is a constant matrix (if all the state variables are measured, C is an identity matrix). To estimate the state variables from noisy measurements, we construct a T-S fuzzy observer as

$$\begin{aligned}\dot{\hat{x}}&=\sum_{i=1}^{2}h_i(\Delta r)[A_i\hat{x}+B_2\bar{u}+L_i(y-\hat{y})]\\ \hat{y}&=C\hat{x}\end{aligned} \tag{13}$$

where $\hat{x}$ is observer state vector, L_i is observer gain matrix to be designed, $\hat{y}$ is observer output.
By defining the estimation error

$$e=x-\hat{x} \tag{14}$$

we obtain

$$\dot{e}=\dot{x}-\dot{\hat{x}}=\sum_{i=1}^{2}h_i(\Delta r)[(A_i-L_iC)e+B_{1i}w-L_in] \tag{15}$$

To making the estimation error as small as possible, we define one control output as

$$z_o=C_ee \tag{16}$$

where C_e is constant matrix. The objective of observer design is to find L_i such that the H_∞ norm of $\|T_{ow}\|$, which denotes the closed-loop transfer function from the steering input w to the control output z_o (estimation error e) and is defined as

$$\|T_{ow}\|_\infty = \sup_{\|w\|_2\neq 0}\frac{\|z_o\|_2}{\|w\|_2} \tag{17}$$

where $\|z_o\|_2^2=\int_0^\infty z_o^T(t)z_o(t)dt$ and $\|w\|_2^2=\int_0^\infty w^T(t)w(t)dt$, is minimised.

On the other hand, to realise good handling and stability, the sideslip angle and the yaw rate need to be controlled to the desired values. Generally, the desired sideslip angle is given as zero and the desired yaw rate is defined in terms of vehicle speed and steering input angle (Zheng, 2006). For simplicity, we only consider to control sideslip angle as small as possible, which in most cases can also lead to satisfied yaw rate. Thus, we define another control output as

$$z_\beta=C_\beta x \tag{18}$$

where $C_\beta=[1\ 0]$, and the objective is to design a robust T-S fuzzy controller based on the estimated state variables as

$$u=\sum_{i=1}^{2}h_i(\Delta r)K_i\hat{x} \tag{19}$$

where K_i is control gain matrix to be designed, such as the H_∞ norm of $\|T_{\beta w}\|$, which denotes the closed-loop transfer function from the steering input w to the control output z_β, is minimised. Together with control output (16), the control output for both observer and controller design is defined as

$$\tilde{z}=\tilde{C}_z\tilde{x}=\begin{bmatrix}C_\beta & C_\beta\\ 0 & C_e\end{bmatrix}\begin{bmatrix}\hat{x}\\ e\end{bmatrix} \tag{20}$$

where $\tilde{x}=[\hat{x}^T\ e^T]^T$ is the augmented system state vector. It can be seen from (20) that C_e can be used to make the compromise between z_β and z_o in the control objective.

To derive the conditions for obtaining K_i and L_i, we now define a Lyapunov function as

$$V=\hat{x}^TP\hat{x}+e^TQe \tag{21}$$

where $P=P^T>0$, $Q=Q^T>0$. Taking the time derivative of V along (13) and (15) yields

$$
\begin{aligned}
\dot{V}&=\dot{\hat{x}}^T P\hat{x}+\hat{x}^T P\dot{\hat{x}}+\dot{e}^T Qe+e^T Q\dot{e}\\
&=\sum_{i=1}^{2} h_i \begin{Bmatrix} 2\left[A_i x+B_2\dfrac{1+\varepsilon}{2}u+B_2\left(\bar{u}-\dfrac{1+\varepsilon}{2}u\right)+L_i Ce+L_i n\right]^T P\hat{x} \\ +2\left[(A_i-L_i C)e+B_{1i}w-L_i n\right]^T Qe \end{Bmatrix}\\
&\le \sum_{i=1}^{2} h_i \begin{Bmatrix} 2\left[A_i x+B_2\dfrac{1+\varepsilon}{2}u+L_i Ce+L_i n\right]^T P\hat{x}+2\left[(A_i-L_i C)e+B_{1i}w-L_i n\right]^T Qe \\ +\kappa\left(u-\dfrac{1+\varepsilon}{2}u\right)^T\left(u-\dfrac{1+\varepsilon}{2}u\right)+\kappa^{-1}\hat{x}^T PB_2B_2^T P\hat{x} \end{Bmatrix}\\
&\le \sum_{i=1}^{2} h_i \begin{Bmatrix} 2\left[A_i x+B_2\dfrac{1+\varepsilon}{2}u+L_i Ce+L_i n\right]^T P\hat{x}+2\left[(A_i-L_i C)e+B_{1i}w-L_i n\right]^T Qe \\ +\kappa\left(\dfrac{1-\varepsilon}{2}\right)^2 u^T u+\kappa^{-1}\hat{x}^T PB_2B_2^T P\hat{x} \end{Bmatrix} \qquad (22)\\
&=\sum_{i=1}^{2} h_i \begin{Bmatrix} \hat{x}^T\left[A_i^T P+PA_i+\left(\dfrac{1+\varepsilon}{2}B_2K_i\right)^T P+\dfrac{1+\varepsilon}{2}PB_2K_i+\kappa\left(\dfrac{1-\varepsilon}{2}\right)^2 K_i^T K_i+\kappa^{-1}PB_2B_2^T P\right]\hat{x}(t) \\ +e^T\left[(A_i-L_i C)^T Q+Q(A_i-L_i C)\right]e+\hat{x}^T PL_i Ce+e^T C^T L_i^T P\hat{x} \\ +w^T B_{1i}^T Qe+e^T QB_{1i}w+\hat{x}^T PL_i n+n^T L_i^T P\hat{x}-e^T QL_i n-n^T L_i^T Qe \end{Bmatrix}\\
&=\sum_{i=1}^{2} h_i\left[\tilde{x}^T\Phi_i\tilde{x}+\tilde{x}^T\Gamma_i\tilde{w}+\tilde{w}^T\Gamma_i^T\tilde{x}\right]
\end{aligned}
$$

where definition (19) and inequalities $X^TY+Y^TX\le\kappa X^TX+\kappa^{-1}Y^TY$ for any matrices X and Y and positive scalar κ (Du et al, 2005) and $\left(\bar{u}-\dfrac{1+\varepsilon}{2}u\right)^T\left(\bar{u}-\dfrac{1+\varepsilon}{2}u\right)\le\left(\dfrac{1-\varepsilon}{2}\right)^2 u^T u$ for any $0<\varepsilon<1$ (Kim & Jabbari, 2002) are applied, and $\tilde{w}=[w^T\ n^T]^T$,

$$
\Phi_i=\begin{bmatrix} A_i^T P+PA_i+\left(\dfrac{1+\varepsilon}{2}B_2K_i\right)^T P+\dfrac{1+\varepsilon}{2}PB_2K_i & PL_iC \\ +\kappa\left(\dfrac{1-\varepsilon}{2}\right)^2 K_i^T K_i+\kappa^{-1}PB_2B_2^T P & \\ * & (A_i-L_iC)^T Q+Q(A_i-L_iC) \end{bmatrix} \qquad (23)
$$

$$
\Gamma_i=\begin{bmatrix} 0 & PL_i \\ QB_{1i} & -QL_i \end{bmatrix} \qquad (24)
$$

By adding $\tilde{z}^T\tilde{z}-\gamma^2 w^T w$ to two sides of (22) yields

$$\begin{aligned}&\dot{V}+\tilde{z}^T\tilde{z}-\gamma^2\tilde{w}^T\tilde{w}\\&\le\sum_{i=1}^{2}h_i\left[\tilde{x}^T\Phi_i\tilde{x}+\tilde{x}^T\Gamma_i\tilde{w}+\tilde{w}^T\Gamma_i^T\tilde{x}+\tilde{x}^T\tilde{C}_z^T\tilde{C}_z\tilde{x}-\gamma^2\tilde{w}^T\tilde{w}\right]\\&=\sum_{i=1}^{2}h_i\bar{x}^T\Theta_i\bar{x}\end{aligned}\tag{25}$$

where $\bar{x}=[\tilde{x}^T\ \tilde{w}^T]^T$, and

$$\Theta_i=\begin{bmatrix}A_i^TP+PA_i+\left(\frac{1+\varepsilon}{2}B_2K_i\right)^TP+\frac{1+\varepsilon}{2}PB_2K_i & PL_iC+C_\beta^TC_\beta & 0 & PL\\ +\kappa\left(\frac{1-\varepsilon}{2}\right)^2K_i^TK_i+\kappa^{-1}PB_2B_2^TP+C_\beta^TC_\beta & & & \\ * & (A_i-L_iC)^TQ+Q(A_i-L_iC) & QB_{1i} & -QL\\ & +C_e^TC_e+C_\beta^TC_\beta & & \\ * & * & -\gamma^2 & 0\\ * & * & * & -\gamma^2\end{bmatrix}\tag{26}$$

It can inferred from (25) that if $\Theta_i<0$, then $\dot{V}+\tilde{z}^T\tilde{z}-\gamma^2\tilde{w}^T\tilde{w}<0$. Thus, the closed-loop system augmented by (13) and (15) is stable when the disturbance $\tilde{w}=0$ and the H_∞ performance on $\|T_{\tilde{z}w}\|$ is satisfied when $\tilde{x}(0)=0$.
By the Schur complement, $\Theta_i<0$ is equivalent to

$$\begin{bmatrix}A_i^TP+PA_i+\left(\frac{1+\varepsilon}{2}B_2K_i\right)^TP+\frac{1+\varepsilon}{2}PB_2K_i & PL_iC+C_\beta^TC_\beta\\ +\kappa\left(\frac{1-\varepsilon}{2}\right)^2K_i^TK_i+\kappa^{-1}PB_2B_2^TP+C_\beta^TC_\beta & \\ * & (A_i-L_iC)^TQ+Q(A_i-L_iC)\\ & +C_e^TC_e+C_\beta^TC_\beta\end{bmatrix}+\gamma^{-2}\begin{bmatrix}0 & PL_i\\ QB_{1i} & -QL_i\end{bmatrix}\begin{bmatrix}0 & PL_i\\ QB_{1i} & -QL_i\end{bmatrix}^T<0\tag{27}$$

which can be written as

$$\begin{bmatrix}\Omega_{11} & \Omega_{12}\\ * & \Omega_{22}\end{bmatrix}<0\tag{28}$$

where

$$\begin{aligned}\Omega_{11}&=A_i^TP+PA_i+\left(\frac{1+\varepsilon}{2}B_2K_i\right)^TP+\frac{1+\varepsilon}{2}PB_2K_i+\kappa\left(\frac{1-\varepsilon}{2}\right)^2K_i^TK_i+\kappa^{-1}PB_2B_2^TP\\&\quad+C_\beta^TC_\beta+\gamma^{-2}PL_iL_i^TP\\\Omega_{12}&=PL_iC+C_\beta^TC_\beta-\gamma^{-2}PL_iL_i^TQ\\\Omega_{22}&=(A_i-L_iC)^TQ+Q(A_i-L_iC)+C_e^TC_e+C_\beta^TC_\beta+\gamma^{-2}Q(B_{1i}B_{1i}^T+L_iL_i^T)Q\end{aligned}\tag{29}$$

It is noted from (28) that P, Q, K_i, L_i, and κ are unknown parameters in the inequality that need to be determined. Because they are coupled together, no effective algorithms for solving them simultaneously can be found by now. Therefore, a two-step procedure is applied. Note that (28) means that $\Omega_{22} < 0$. So, in the first step, we solve $\Omega_{22} < 0$. By defining $X_i = QL_i$ and using the Schur complement, from $\Omega_{22} < 0$, we obtain

$$\begin{bmatrix} A_i^T Q^T - C^T X_i^T + QA_i - X_i C + C_\beta^T C_\beta & C_e^T & QB_{1i} & X_i \\ * & -I & 0 & 0 \\ * & * & -\gamma^2 I & 0 \\ * & * & * & -\gamma^2 I \end{bmatrix} < 0 \tag{30}$$

which are LMIs and can be solved by means of the Matlab LMI Toolbox software. Then, we can obtain L_i by using $L_i = Q^{-1}X_i$ for a given γ.

In the second step, by defining $W = P^{-1}$, pre- and post-multiplying (28) by $\mathrm{diag}(W\ I)^T$ and its transpose, respectively, we obtain

$$\begin{bmatrix} WA_i^T + A_i W + W\left(\frac{1+\varepsilon}{2}B_2 K_i\right)^T + \frac{1+\varepsilon}{2}B_2 K_i W & L_i C + WC_\beta^T C_\beta - \gamma^{-2} L_i L_i^T Q \\ +\gamma^{-2} L_i L_i^T + \kappa\left(\frac{1-\varepsilon}{2}\right)^2 WK_i^T K_i W + \kappa^{-1} B_2 B_2^T + WC_\beta^T C_\beta W & \\ & \Omega_{22} \end{bmatrix} < 0 \tag{31}$$

After defining $Y_i = K_i W$ and using the Schur complement, we obtain

$$\begin{bmatrix} WA_i^T + A_i W + \frac{1+\varepsilon}{2}B_2 Y_i + \frac{1+\varepsilon}{2}Y_i B_2 & WC_\beta^T & L_i C + WC_\beta^T C_\beta \\ +\kappa\left(\frac{1-\varepsilon}{2}\right)^2 Y_i^T Y_i + \kappa^{-1} B_2 B_2^T + \gamma^{-2} L_i L_i^T & & -\gamma^{-2} L_i L_i^T Q \\ * & -I & 0 \\ * & * & \Omega_{22} \end{bmatrix} < 0 \tag{32}$$

which are LMIs and can be solved by means of the Matlab LMI Toolbox software to obtain $K_i = Y_i W^{-1}$ for a given γ.

On the other hand, from (19), the constraint

$$\left| \sum_{i=1}^{2} h_i(\Delta r) K_i \hat{x} \right| \le \frac{u_{\lim}}{\varepsilon} \tag{33}$$

can be expressed as $\left|K_i \hat{x}\right| \le \frac{u_{\lim}}{\varepsilon}$.

Let $\Psi(K_i)=\left\{\hat{x}\left|\left\|\hat{x}K_i^T K_i\hat{x}\right\|\le\left(\frac{u_{lim}}{\varepsilon}\right)^2\right.\right\}$, the equivalent condition for an ellipsoid $\Psi(P,\rho)=\left\{\hat{x}\left|\left\|\hat{x}^T P x\le\rho\right\|\right.\right\}$ being a subset of $\Psi(K_i)$, i.e., $\Psi(P,\rho)\subset\Psi(K_i)$, is given as (Cao & Lin, 2003)

$$K_i\left(\frac{P}{\rho}\right)^{-1}K_i^T\le\left(\frac{u_{lim}}{\varepsilon}\right)^2 \tag{34}$$

By the Schur complement, inequality (34) can be written as

$$\begin{bmatrix}\left(\frac{u_{lim}}{\varepsilon}\right)^2 I & K_i\left(\frac{P}{\rho}\right)^{-1}\\ * & \left(\frac{P}{\rho}\right)^{-1}\end{bmatrix}\ge 0 \tag{35}$$

Using the definitions $W = P^{-1}$ and $Y_i = K_i W$, inequality (35) is equivalent to

$$\begin{bmatrix}\left(\frac{u_{lim}}{\varepsilon}\right)^2 I & Y_i\\ * & \rho^{-1}W\end{bmatrix}\ge 0 \tag{36}$$

In summary, the procedure for the observer based robust controller design is given as: (1) give initial value for γ; (2) solve LMIs (30), (32), and (36) to obtain L_i and K_i; (3) decrease γ and repeat the previous two steps until no feasible solutions can be found; (4) construct the observer and controller in terms of L_i and K_i.

4. Numerical simulations

To evaluate the effectiveness of the proposed observer based controller design approach, numerical simulations on a yaw-plane 2DOF vehicle dynamics model with nonlinear Dugoff tyre model will be done in this section. The parameters used for the vehicle model are given as m=1298.9 kg, I_z=1627 kg.m^2, l_f=1.0 m, l_r=1.454 m. The robust observer based controller is designed using the above introduced approach, where C_f= C_r =60000 N.rad^{-1} is used when tyre sideslip angle is in linear region and C_f= C_r =6000 N.rad^{-1} is used when tyre sideslip angle is in nonlinear region, and the saturation limit is assumed as 3000 Nm, i.e., u_{lim}=3000 Nm. By choosing ε =0.024, ρ =9.8, we obtain the controller matrices as $K_1=10^4$[2.2258 -2.6083] and $K_2=10^4$[-1.1797 -1.6864], and observer gain matrices as L_1=[8.1763 165.4576] and L_2=[8.4599 162.6120].

To testify the vehicle lateral dynamics performance, a J-turn manoeuvre, which is produced from the ramp steering input (the maximum degree is 6 deg), is used. To validate the effectiveness of the designed observer based controller, we first assume the vehicle is driving on a snow surface road (road friction is assumed as 0.5) with forward velocity 20 m/s, and only yaw rate is measurable without measurement noise. To see the observer performance clearly, we define different initial values for the vehicle model and observer. Fig. 3 shows sideslip angle responses under J-turn manoeuvre for the uncontrolled system

(without any controller), the controlled system (with the designed controller), and the sideslip angle observer.

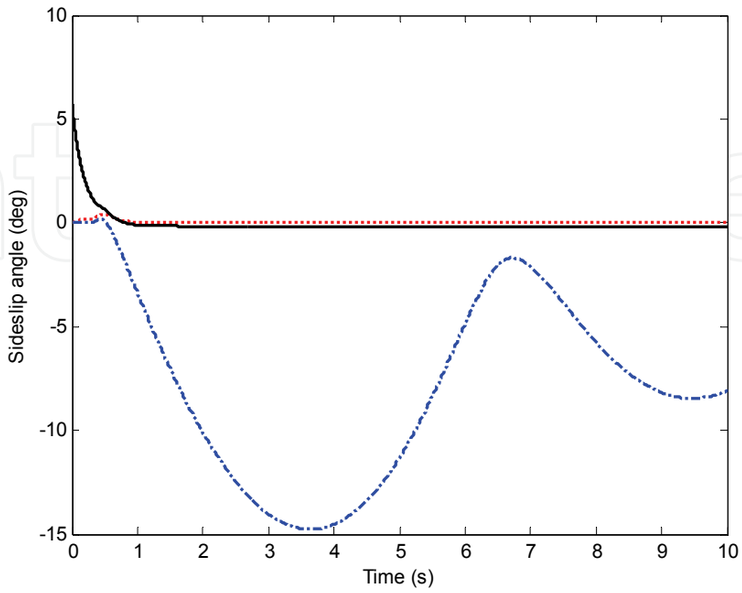

Fig. 3. Sideslip angle responses under J-turn manoeuvre on a snow road without measurement noise. Dashed-dotted line is sideslip angle for uncontrolled system. Dotted line is sideslip angle for controlled system with the designed controller, and solid line is sideslip angle estimated from observer.

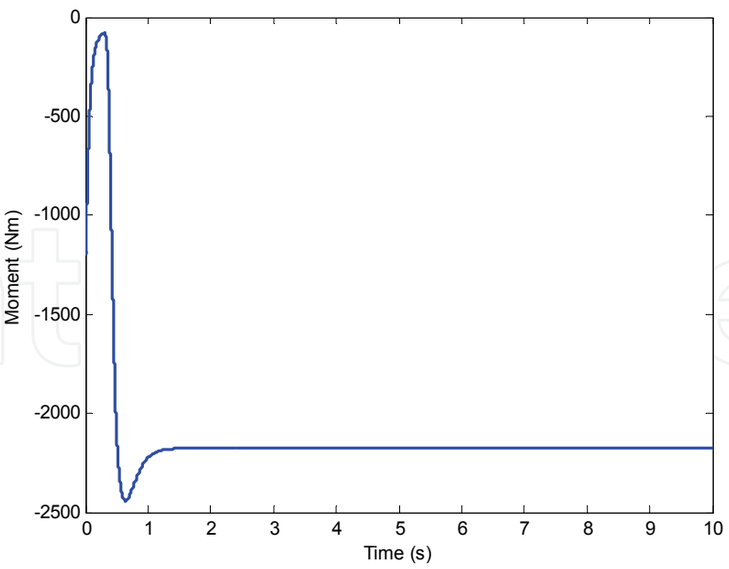

Fig. 4. Yaw moment under J-turn manoeuvre on a snow road without measurement noise.

It can be seen from Fig. 3 that the sideslip angle of the controlled system converges to the desired sideslip value, zero degree. On the contrary, the sideslip angle of the uncontrolled system is big which may cause vehicle unstable motion (Mirzaei, 2010). It is also observed

from Fig. 3 that the estimated sideslip angle is converging to the real sideslip angle quickly even though there is big difference on the initial values of observer and vehicle model. Fig. 4 shows the required yaw moment, which is within the defined saturation limit. As demonstrated by the simulation results, the designed observer based controller effectively improves the vehicle handling and stability performance with using yaw rate measurement.

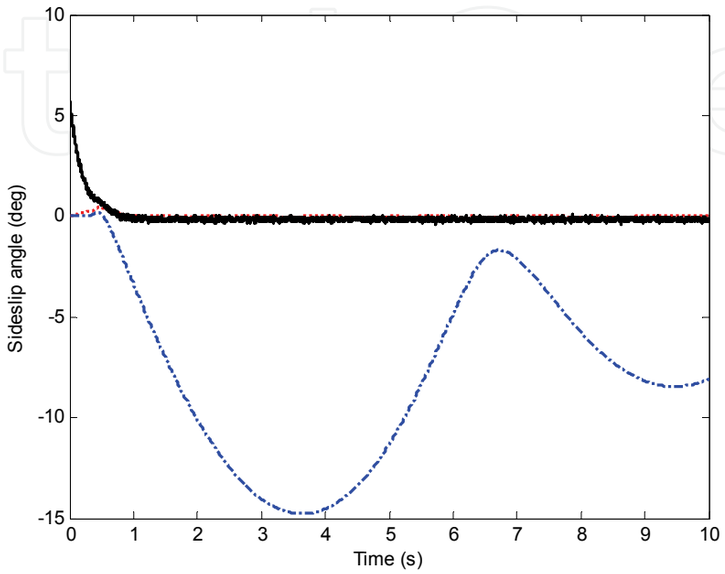

Fig. 5. Sideslip angle responses under J-turn manoeuvre on a snow road with measurement noise. Dashed-dotted line is sideslip angle for uncontrolled system. Dotted line is sideslip angle for controlled system with the designed controller, and solid line is sideslip angle estimated from observer.

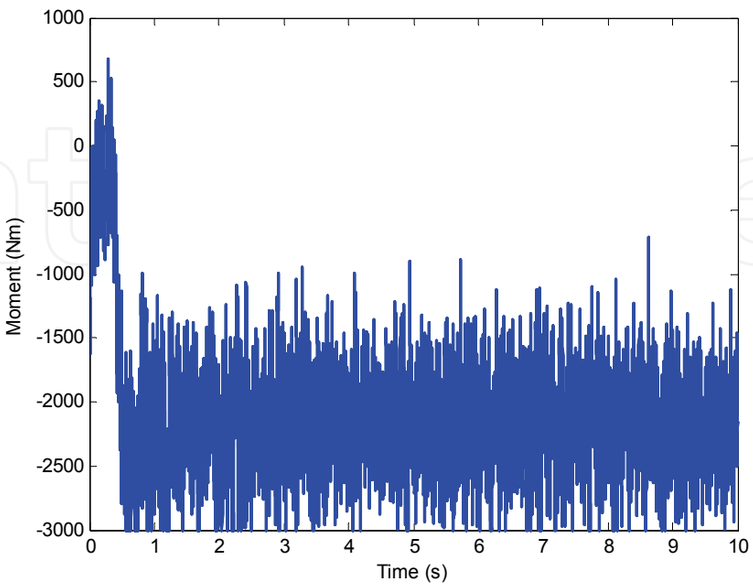

Fig. 6. Yaw moment under J-turn manoeuvre on a snow road with measurement noise.

To validate the robustness of the designed controller, we now add measurement noise on yaw rate. The sideslip angle responses under J-turn manoeuvre for uncontrolled system, controlled system, and observer are shown in Fig. 5. It can been seen from Fig. 5 that the sideslip angle of the controlled system is still approaching to the desired sideslip angle in spite of small effect caused by the measurement noise. The required yaw moment is shown in Fig. 6, where big variations on the yaw moment caused by measurement noise can be observed.

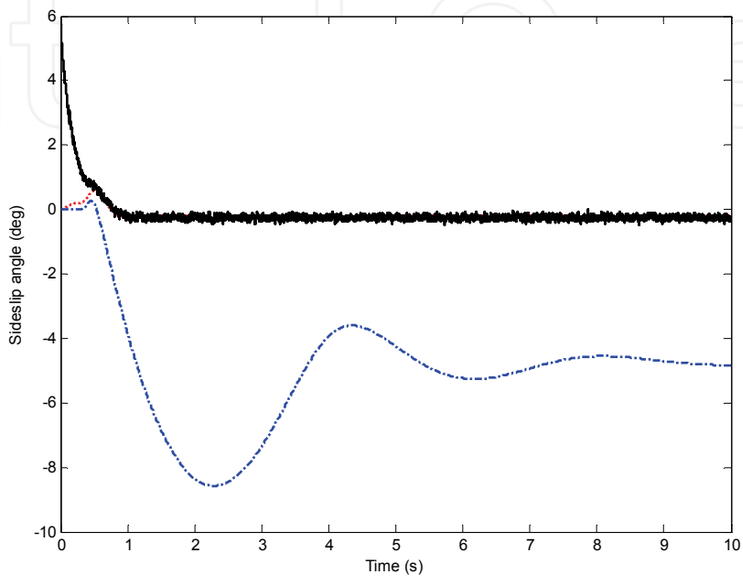

Fig. 7. Sideslip angle responses under J-turn manoeuvre on a dry surface road with measurement noise. Dashed-dotted line is sideslip angle for uncontrolled system. Dotted line is sideslip angle for controlled system with the designed controller, and solid line is sideslip angle estimated from observer.

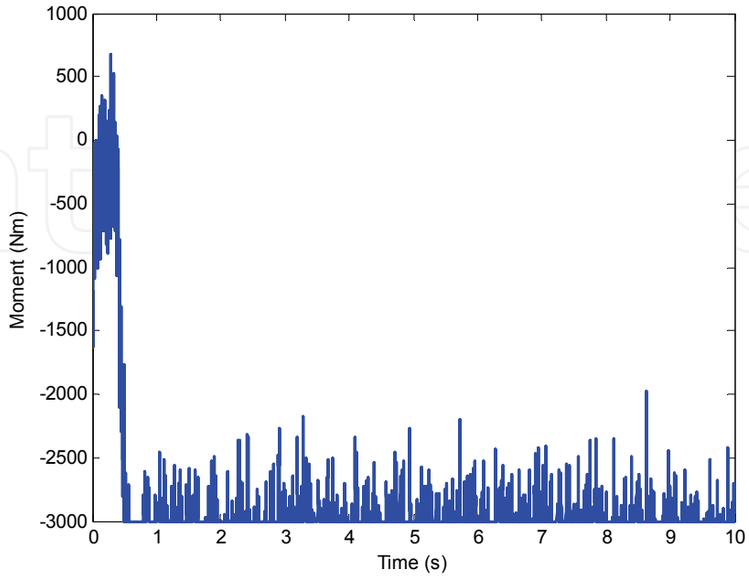

Fig. 8. Yaw moment under J-turn manoeuvre on a dry road with measurement noise.

To further validate the robustness of the designed controller, we now assume the vehicle is driving on a dry surface road (road friction is assumed as 0.9) with forward velocity 20 m/s. The sideslip angle responses and yaw moment are shown in Figs. 7 and 8, respectively. It can be seen the designed controller can achieve good performance with the limited yaw moment no matter the change of road condition.

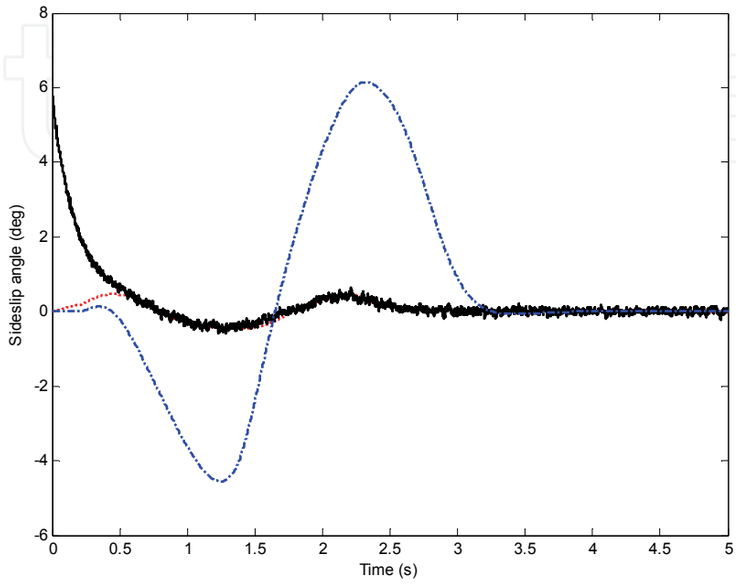

Fig. 9. Sideslip angle responses under lane change manoeuvre on a dry road with measurement noise. Dashed-dotted line is sideslip angle for uncontrolled system. Dotted line is sideslip angle for controlled system with the designed controller, and solid line is sideslip angle estimated from observer.

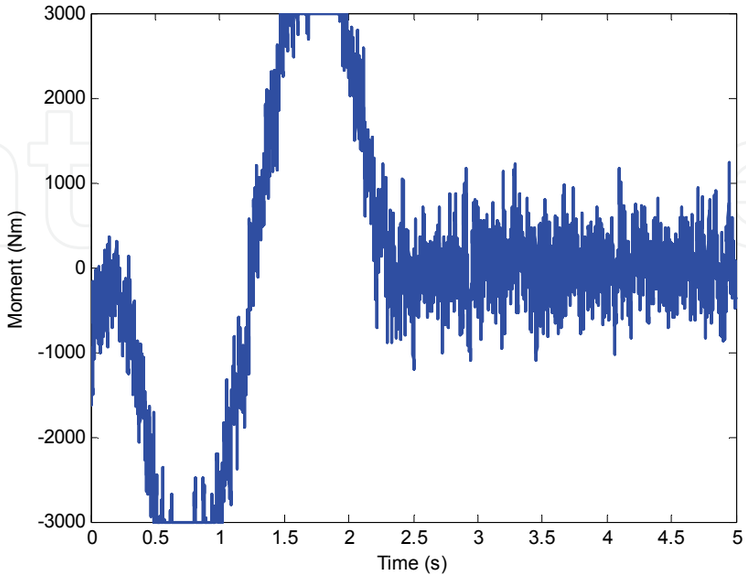

Fig. 10. Yaw moment under lane change manoeuvre on a dry road with measurement noise.

Finally, a lane change manoeuvre is applied to validate the effectiveness of the designed controller. As shown in Fig. 9 on sideslip angle and Fig. 10 on yaw moment, similar conclusion can be obtained on the performance achieved by the designed controller.

5. Conclusion

In this chapter, the practical design of a robust direct yaw moment controller for vehicle to improve lateral dynamics stability and handling with considering tyre cornering stiffness uncertainties, actuator saturation, measurement noise, and estimation of sideslip angle is studied. A two-step procedure is used to solve the observer and controller design problem, which can further be expressed as LMIs and can be solved very efficiently using currently available software like Matlab LMI Toolbox. Numerical simulations are applied to check the performance of the designed controller. The results show that the designed controller can improve vehicle handling and stability regardless of the measurement noise, changes of road conditions and manoeuvres. Further study on this topic will consider parameter uncertainties such as mass, moment of inertia, and forward velocity, etc., and study the reflection of road friction on vehicle model with choosing the most appropriate premise variables and defining the optimal membership functions.

6. References

Abe, M. (1999). Vehicle dynamics and control for improving handling and active safety: from four-wheel steering to direct yaw moment control, *Proc. Instn. Mech. Engrs. Part K: J. Multi-body Dynamics* Vol. 213, 87-101

Antonov, S., Fehn, A. and Kugi, A. (2008). A new flatness-based control of lateral vehicle dynamics, *Vehicle System Dynamics* Vol. 46, No. 9, 789-801

Boada, B. L., Boada, M. J. L. and Diaz, V. (2005). Fuzzy-logic applied to yaw moment control for vehicle stability, *Vehicle System Dynamics* Vol. 43, No. 10, 753-770

Canale, M., Fagiano, L., Milanese, M. and Borodani, P. (2007). Robust vehicle yaw control using an active differential and IMC techniques, *Control Engineering Practice* Vol. 15, 923-941

Cao, Y.-Y. and Lin, Z. (2003). Robust stability analysis and fuzzy-scheduling control for nonlinear systems subject to actuator saturation, *IEEE Transactions on Fuzzy Systems* 11(1): 57-67

Du, H., Lam, J. and Sze, K. Y. (2005). H∞ disturbance attenuation for uncertain mechanical systems with input delay, *Transactions of the Institute of Measurement and Control* 27(1): 37-52

Esmailzadeh, E., Goodarzi, G. R. and Vossoughi, G. R. (2003). Optimal yaw moment control law for improved vehicle handling, *Mechatronics* Vol. 13, 659-675

Fukada, Y. (1999). Slip-angle estimation for vehicle stability control, *Vehicle System Dynamics*, Vol. 32, 375-388

Kim, J. H. and Jabbari, F. (2002). Actuator saturation and control design for buildings under seismic excitation, *Journal of Engineering Mechanics* Vol. 128, No. 4, 403-412.

Li, B. and Yu, F. (2010). Design of a vehicle lateral stability control system via a fuzzy logic control approach, *Proc. Instn. Mech. Engrs. Part D: J. Automobile Engineering* Vol. 224, 313-326.

Mirzaei, M., Alizadeh, G., Eslamian, M. and Azadi, S. (2008). An optimal approach to nonlinear control of vehicle yaw dynamics, *Proc. Instn. Mech. Engrs. Part I: J. Systems and Control Engineering* Vol. 222, 217-229.

Mirzaei, M. (2010). A new strategy for minimum usage of external yaw moment in vehicle dynamic control system, *Transportation Research Part C: Emerging Technologies* Vol. 18, No. 2, 213–224.

Tanaka, K. andWang, H. O. (2001). *Fuzzy control systems design and analysis: A linear matrix inequality approach*, John Wiley & Sons, Inc., New York.

Yang, X., Wang, Z. and Peng, W. (2009). Coordinated control of AFS and DYC for vehicle handling and stability based on optimal guaranteed cost theory, *Vehicle System Dynamics,* Vol. 47, No. 1, 57-79

Zheng, S.; Tang, H., Han, Z. and Zhang, Y. (2006). Controller design for vehicle stability enhancement, *Control Engineering Practice,* Vol. 14, 1413-1421

Robust Control, Theory and Applications

Edited by Prof. Andrzej Bartoszewicz

ISBN 978-953-307-229-6
Hard cover, 678 pages
Publisher InTech
Published online 11, April, 2011
Published in print edition April, 2011

The main objective of this monograph is to present a broad range of well worked out, recent theoretical and application studies in the field of robust control system analysis and design. The contributions presented here include but are not limited to robust PID, H-infinity, sliding mode, fault tolerant, fuzzy and QFT based control systems. They advance the current progress in the field, and motivate and encourage new ideas and solutions in the robust control area.

InTech Europe
University Campus STeP Ri
Slavka Krautzeka 83/A
51000 Rijeka, Croatia
Phone: +385 (51) 770 447
Fax: +385 (51) 686 166
www.intechopen.com

InTech China
Unit 405, Office Block, Hotel Equatorial Shanghai
No.65, Yan An Road (West), Shanghai, 200040, China
中国上海市延安西路65号上海国际贵都大饭店办公楼405单元
Phone: +86-21-62489820
Fax: +86-21-62489821

IntechOpen